

# Development of a Cost-Effective 1.5kN Liquid-Fueled Rocket Propulsion System

Jason Chen <sup>\*1</sup>, Srikar Gouri <sup>†2</sup>, Sophia Troshynski <sup>‡3</sup>, Ron Nachum <sup>§4</sup>, and Ankit Khandelwal <sup>¶5</sup>

<sup>1</sup>*Project Lead and Chief Engineer*, <sup>2</sup>*Flight and Ground Software Lead*, <sup>3</sup>*Manufacturing and Structures Lead*, <sup>4</sup>*Propulsion Lead*, <sup>5</sup>*Avionics Lead*



Project Caelus, 501(c)(3)  
(Initial revision 06 August, 2019; received 26 March, 2020)

This is an example of the abstract. Mit der CNN.com Europe Edition verfügt der TV-Sender CNN über eine umfassende Webseite, die im Minutentakt rund um die Uhr aktualisierte Weltnachrichten aus einer europäischen Perspektive auf den Bildschirm bringt. Wichtige, globale Ereignisse, geordnet in den Rubriken breaking news, current news headlines oder in depth, werden mit Hilfe von Video- und Audioclips, Bildern, Karten, Profilen, Zeitachsen und Tatsachenberichten fundiert dargestellt. Die Nachrichten stützen sich auf die Expertenanalysen der CNN Korrespondenten. Die Berichte verweisen auf andere relevante CNN Reportagen und zu Meldungen anderer Websites. Zusätzlich besteht die Möglichkeit, Videos anzufordern und mittels einer Suchfunktion Zugriff auf bereits gesendete Berichte und gesonderte Themenbereiche, die seit 1995 bearbeitet wurden, zu erhalten.

## 1 Nomenclature

### Symbols

$\epsilon$	=	Expansion ratio	
$\gamma$	=	Ratio of specific heats	
$\rho$	=	Density	$g/cm^3$
$C^*$	=	Characteristic velocity	$m/s$
$C_d$	=	Discharge coefficient	
$C_v$	=	Valve flow coefficient	
$f_d$	=	Friction factor	
$F_t$	=	Thrust	$N$
$g_0$	=	Acceleration due to gravity	$m/s^2$
$I_{sp}$	=	Specific impulse	$s$
$\dot{m}$	=	Mass flow rate	$kg/s$
$O/F$	=	Oxidizer-to-fuel ratio	
$Q$	=	Volumetric flow rate	$L/s$

### Acronyms

$CEA$	=	Chemical equilibrium with applications
$COTS$	=	Commercial off-the-shelf
$DAQ$	=	Data acquisition & control
$FOD$	=	Foreign object debris
$GLOW$	=	Gross lift-off weight
$MECO$	=	Main engine cut-off
$P\&ID$	=	Plumbing and instrumentation diagram
$PT$	=	Pressure transducer
$TC$	=	Thermocouple
$SF$	=	Safety factor
$VDC$	=	Direct current voltage

\*jay.chen135@gmail.com, contact@projectcaelus.org

†srikarg89@gmail.com

‡stroshynski@gmail.com

§ronnachum13@gmail.com

¶amtron521@gmail.com

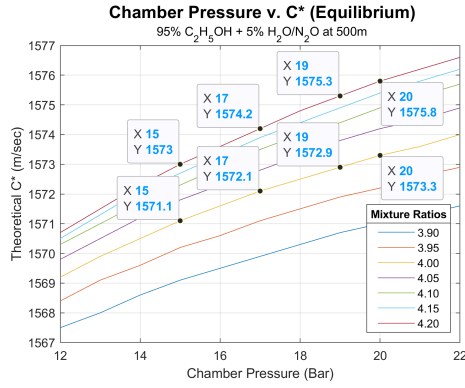


Figure 1: Theoretical C\* efficiency vs chamber pressure and numerous mixture ratios.

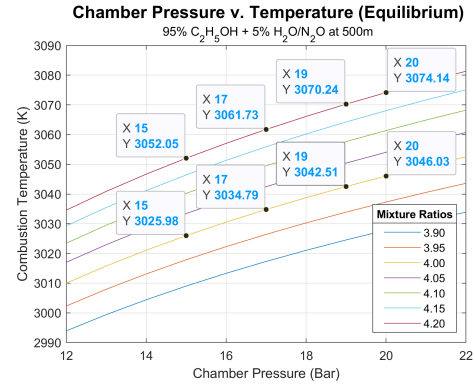


Figure 2: Combustion temperature vs chamber pressure and numerous mixture ratios.

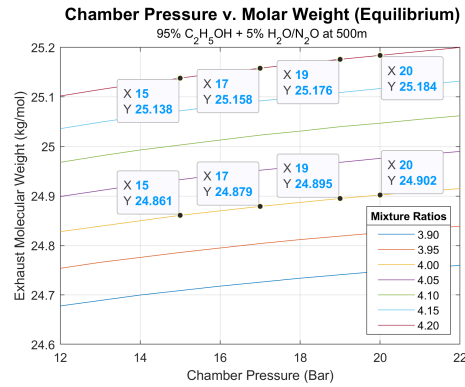


Figure 3: Gas molecular mass vs chamber pressure and numerous mixture ratios.

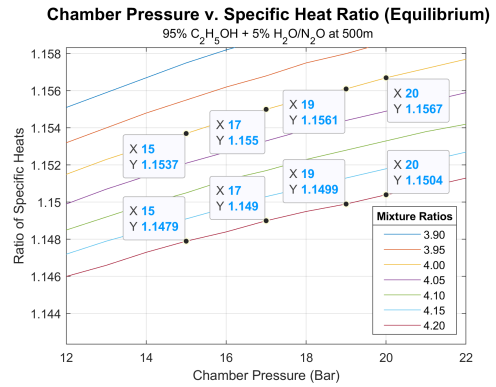


Figure 4: Ratio of specific heats vs chamber pressure and numerous mixture ratios.

Note: Subscripts follow the convention outlined in [3]. Unless otherwise specified, subscript 0 indicates at stagnation or impact conditions, 1 indicates conditions at the nozzle inlet or combustion chamber,  $t$  indicates the nozzle throat, 2 is at the nozzle exit, and 3 is at ambient conditions.

## 2 Initial System Characterization

Project Caelus' unique position as a 501(c)(3) non-profit organization consisting entirely of high school students has laid the foundation for a design approach fully committed to cost-effectiveness, simplicity, and reliability. The following section outlines the initial design choices made for our overall system and reflects our emphasis on the aforementioned ideals.

### 2.1 Objectives

The Callisto 1 system is set to the following constraints and objectives:

1. Reach an altitude of 1500 m ( $\approx$  5000 ft).
2. A *GLOW* of no more than 30 kg ( $\approx$  70 lbsm).
3. A nominal main engine thrust of 1.5 kN ( $\approx$  350 lbf).
4. A chamber pressure in the range of around 15 Bar to 20 Bar ( $\approx$  218 psi to 300 psi)
5. Consume a budget of no more than \$10,000 USD.
6. Utilize 95% ethyl alcohol and nitrous oxide as the propellant combination.

## 2.2 Chamber Pressure and Mixture Ratio Selection

The first step is to realize the theoretical maximum performance to be expected from our propellant combination. 95% ethyl alcohol (ethanol) was chosen for its availability, low pricing, and a modest specific impulse. A 95% dilution (by mass) with water was chosen as to lower the expected combustion chamber temperature. This trade-off sacrifices some  $I_{sp}$  but reduces engineering complexity as regenerative and film cooling circuits may not be required. Industrial nitrous oxide was chosen as the main oxidizer for its self-pressurizing characteristics, non-cryogenic nature as opposed to liquid oxygen, relative ease to obtain, and a modest  $I_{sp}$  with ethanol. Using CEA, an open-source thermodynamics library provided by NASA’s Glenn Research Center, critical data describing propellant combustion characteristics could be obtained. Numerical Python scripts were written to iterate through various combustion chamber pressures and mixture ratios and interface with CEA, and MATLAB scripts were used to parse and graph the CEA outputs as shown in Figures 1, 2, 3, and 4. Mixture ratios of 4.0 and 4.2 are labeled at certain chamber pressures. All dependent-variable properties (characteristic velocity  $C^*$ , combustion temperature  $T_c$ , exhaust molar mass  $M$ , and exhaust specific heat ratio  $\gamma$ ) were permuted assuming shifting equilibrium flow and at an operational altitude of 500 m.

A mixture ratio of 4.0 was chosen for Aphlex 1B mainly in the interest of a conservative combustion temperature of around 3026 K and a middle-of-the-line theoretical  $C^*$  of around 1570 m/s, given a chamber pressure of 15 bar. This chamber pressure was chosen to minimize upstream fluid pressures and thus tank weight requirements, while also considering two additional design constraints that were not mentioned above but are nevertheless valid guiding parameters: a fluid flow velocity of less than 6 m/s to avoid water hammer effects [Zucrow Laboratories] and a pressure drop across the injector of around 25% of the designated chamber pressure [Michigan Aeronautical Science Association]. The former of these additional guidelines is to avoid feed-coupled combustion instabilities that may be observed when the  $\delta p$  across the injector is not adequately high. These guidelines further encourage a lower chamber pressure, and thus a conservative value of 15 Bar was chosen.

## 3 Propulsion System Design

The following section outlines the design process for Aphlex 1B, our second-generation bi-propellant liquid rocket engine, set to fly on our 30 kg launch vehicle, Callisto 1, given the objectives and data obtained in the previous section.

### 3.1 Nozzle Design

Design Parameters			
Name	Value	Unit	Uncertainty
Propellant (Fuel)	Ethanol ( $C_2H_5OH$ , 95%)	N/A	N/A
Propellant (Oxidizer)	Nitrous oxide ( $N_2O$ )	N/A	N/A
$O/F$ , Oxidizer/fuel ratio	4.0	N/A	$\pm 1\%$
$F_t$ , Nominal thrust	1.50	kN	$\pm 0.1\%$
$P_c$ , Chamber static pressure	$1.5 \times 10^6$	Pa	$\pm 0.1\%$
$P_e$ , Ambient pressure	$9.5540 \times 10^4$	Pa	$\pm 0.1\%$
$T_c$ , Chamber static temperature	3025.98	K	$\pm 0.01\%$
$M$ , Exhaust molecular mass	24.861	kg/mol	$\pm 0.01\%$
$\gamma$ , Specific heat ratio	1.1537	N/A	$\pm 0.001\%$

Table 1: Summary of exhaust gas properties and fluid parameters.

$$T_3 = 15.04 - 0.00649h \quad (3.1)$$

$$P_3 = \left[ 101.29 \times \left( \frac{T + 273.1}{288.08} \right)^{5.256} \right] \times 1000 \quad (3.2)$$

The nozzle design process followed standard procedures outlined in Rocket Propulsion Elements [3] and open-source NASA documents. The thermodynamic properties of the exhaust gas and other important parameters are summarized and compiled in Table 1. The ambient pressure was calculated

using NASA Glenn Research Center's Earth Atmosphere Model for an altitude within the troposphere (less than 11000 meters), as shown in Equations 3.1 and 3.2, where  $T_3$  represents the ambient temperature in Kelvin,  $h$  is the altitude in meters,  $P_3$  is the ambient pressure in Pascals.

Assuming fully isentropic flow (by definition both adiabatic and reversible) in the supersonic nozzle with choked flow conditions at the throat, an ideal converging-diverging (de Laval) nozzle can be characterized. The first parameter to calculate is the controlling area ratio

$$\frac{A_t}{A_2} = \left(\frac{\gamma+1}{2}\right)^{1/(\gamma-1)} \left(\frac{p_2}{p_1}\right)^{1/\gamma} \sqrt{\frac{\gamma+1}{\gamma-1} \left[1 - \left(\frac{p_2}{p_1}\right)^{(\gamma-1)/\gamma}\right]} \quad (3.3)$$

where  $A_t$  is the cross-sectional area of the throat,  $A_2$  is the cross-sectional area at nozzle exit, and  $p_1$  and  $p_2$  are the chamber pressure and exit pressure respectively. Equation 3.3 is also often referred to as the inverse of the expansion ratio  $\epsilon$ , since  $\epsilon = A_2/A_t$ . Evaluating Equation 3.3 gives

$$\frac{A_t}{A_2} = \left(\frac{2.15}{2}\right)^{1/0.15} \left(\frac{9.6 \times 10^4}{1.5 \times 10^6}\right)^{1/1.15} \sqrt{\frac{2.15}{0.15} \left[1 - \left(\frac{9.6 \times 10^4}{1.5 \times 10^6}\right)^{0.15/1.15}\right]} = 0.307$$

Notice the substitution of  $p_2$  for  $P_e$  as specified in Table 1, since in an ideal nozzle, the exhaust gas should expand to ambient pressure. The expansion ratio  $\epsilon$  is simply

$$\epsilon = A_2/A_t = 1/AR = 1/0.307 = 3.26$$

Next, we can find the ideal exit velocity  $v_2$ , sometimes denoted as  $c$ :

$$v_2 = \sqrt{\frac{2\gamma}{\gamma-1} \left(\frac{R_u T_1}{M}\right) \left[1 - \left(\frac{p_2}{p_1}\right)^{(\gamma-1)/\gamma}\right]} \quad (3.4)$$

where  $R_u$  is the universal gas constant of 8314.3 J/kg mol-K and  $M$  is the molecular mass of the gas as shown in Table 1. Evaluating gives

$$v_2 = \sqrt{\frac{2 * 1.15}{0.15} \left(\frac{8314.3 * 3026}{24.86}\right) \left[1 - \left(\frac{9.6 \times 10^4}{1.5 \times 10^6}\right)^{0.15/1.15}\right]} = 2162.3 \text{ m/s}$$

Next, the mass flow rate  $\dot{m}$  can be calculated explicitly noting that  $v_2 = c$ , since earlier it was stated that  $p_2 = p_3$ :

$$\dot{m} = F_t/c = 1500/2162.3 = 0.694 \text{ kg/s} \quad (3.5)$$

Solving using our chosen  $O/F$  ratio of 4.0 for each independent propellant  $\dot{m}$  gives

$$\begin{aligned} \dot{m}_o &= \dot{m} * (4/5) = 0.694 * (4/5) = 0.555 \text{ kg/s} \\ \dot{m}_f &= \dot{m} * (1/5) = 0.694 * (1/5) = 0.139 \text{ kg/s} \end{aligned}$$

Next, we arrive at the throat area:

$$A_t = \frac{\dot{m}}{p_1} \sqrt{\frac{(R_u/M)T_1}{\gamma[2/(\gamma+1)]^{(\gamma+1)/(\gamma-1)}}} \quad (3.6)$$

Evaluating Equation 3.6 gives

$$A_t = \frac{0.694}{1.5 \times 10^6} \sqrt{\frac{(8314.3/24.86) * 3026}{1.15[2/(2.15)]^{(2.15)/(0.15)}}} = 7.29 \times 10^{-4} \text{ m}^2 = 7.29 \text{ cm}^2$$

Using this calculated throat area and the expansion ratio, the exit area is simply

$$A_2 = \epsilon * A_t = 3.26 * 7.29 \times 10^{-4} = 2.38 \times 10^{-3} \text{ m}^2 = 23.8 \text{ cm}^2 \quad (3.7)$$

From the parameters calculated thus far, we can calculate some useful performance metrics such as  $I_{sp}$  and thrust coefficient  $C_F$ :

$$(I_{sp})_{opt} = F_t/(\dot{m} * g_0) = c/g_0 = 2162.3/9.81 = 220.42 \text{ sec} \quad (3.8)$$

where  $g_0$  is the acceleration due to gravity at Earth's surface.  $C_F$  is

$$(C_F)_{opt} = \frac{F_t}{p_1 A_t} = \frac{1500}{1.5 \times 10^6 * 7.29 \times 10^4} = 1.372 \quad (3.9)$$

Note that under a more rigorous derivation,  $C_F$  can be seen to be a key parameter for analysis and varies depending on  $\gamma$ , the nozzle expansion ratio  $\epsilon$ , and the pressure ratio  $p_1/p_2$ . Normally,  $C_F$  is experimentally determined by measuring chamber pressure, throat diameter, and thrust. The optimal  $C_F$  and therefore  $F_t$  occur when  $p_2 = p_3$ .

Finally, the physical dimensions of the nozzle can be determined using simple trigonometry via a standard convergence half-angle  $\alpha$  of  $45^\circ$  and a standard divergence half-angle  $\beta$  of  $15^\circ$ . The characteristic chamber length  $L^*$ , a parameter used for characterizing the necessary chamber volume for adequate mixing and combustion of the propellants, must be more carefully considered. Ideally,  $L^*$  is purely a function of the chemistry of the propellant combination and is often based upon previous successful engine designs [3]. However, due to the dynamical and complex nature of nitrous oxide, such as exothermic decomposition after vaporization in the injector and a high density sensitivity to temperature, a more sophisticated model is needed to calculate  $L^*$ . Palacz proposes an explicit equation for finding the ideal  $L^*$  for a nitrous oxide system, and empirically determined an ideal range for an  $NO_x$ /ethanol system of  $L^*$  values from 125.6 cm to 167.8 cm [1]. This range is confirmed by Sutton and Biblarz, as  $L^*$  values of between 1.0 m and 1.5 m are expected with ethanol systems. A low-range  $L^*$  value of 1.25 m was chosen as a smaller form factor is desired over perfect combustion efficiency.  $L^*$  is mathematically defined as

$$L^* = \frac{V_c}{A_t} = \frac{\pi r_c^2 L_c}{A_t} \implies L_c = \frac{A_t L^*}{\pi r_c^2} \quad (3.10)$$

where  $L_c$  is the length of the chamber and  $r_c$  is the radius of the chamber. It is apparent that the a desired form factor can be obtained by adjusting either the radius or the length of the chamber. Through iteration, a chamber radius  $r_c$  of 4.0 cm was chosen. The only constraint on the chamber radius is the contraction ratio, defined as  $A_1/A_t$  (the ratio of chamber area to throat area), which must achieve a value of 4.0 or more [3]. A trivial area calculation can be performed to confirm that this constraint is satisfied:  $CR = \pi r_c^2 / A_t = 5.03 \times 10^{-4} \text{ m}^2 / 7.29 \times 10^{-4} \text{ m}^2 = 6.90 > 4.0$ . The chamber length is therefore

$$L_c = \frac{A_t L^*}{\pi r_c^2} = \frac{(7.29 \times 10^{-4} \text{ m}^2)(1.25 \text{ m})}{5.03 \times 10^{-4} \text{ m}^2} = 0.1813 \text{ m} = 18.13 \text{ cm}$$

Calculated Performance Parameters		
Name	Value	Unit
$\dot{m}$ , Total mass flow rate	0.694	kg/s
$\dot{m}_f$ , Fuel mass flow rate	0.555	kg/s
$\dot{m}_o$ , Oxidizer mass flow rate	0.139	kg/s
$v_2$ , Exhaust velocity	2162.3	m/s
$(I_{sp})_{opt}$ , Specific impulse (optimal)	220.42	s
$(C_F)_{opt}$ , Thrust coefficient (optimal)	1.372	N/A

Table 2: Summary of engine performance parameters.

Table 2 shows the calculated engine parameters and Table 3 shows the calculated physical nozzle dimensions. Using the data from Table 3, a basic conical nozzle can be realized.

Figure 5 shows the basic conical nozzle for Aphlex 1B created using the given dimensions. Although a conical nozzle may exhibit an advantage in its ease of manufacturing, it is sub-optimal for performance since 1) the exhaust is not exiting the nozzle completely parallel to the nozzle axis, which results in lateral losses of energy, 2) the sharp convex corner at the throat generates shocks which are not adequately dissipated by a conical nozzle, and 3) the small divergence half-angle ensures a long diverging section, which increases engine mass. To address these issues, most modern nozzles are so-called "bell" nozzles, whose diverging section includes a straightening section to address the first issue and inherently addresses the third issue by having a more rapidly expanding cross-section as compared to conical nozzles. To neutralize the Prandtl-Meyer expansion fans generated at the sharp corner of the throat, a numerical technique called the Method of Characteristics (MOC) is used to generate the nozzle contour.

In brief, MOC propagates characteristic lines emanating from the throat, and by using equations to model characteristic interactions and reflections, it is able to generate a nozzle contour to precisely

Calculated Dimensional Parameters		
Name	Value	Unit
$\alpha$ , Convergence half-angle	45	<i>deg</i>
$\beta$ , Divergence half-angle	15	<i>deg</i>
$A_t$ , Throat area	$7.29 \times 10^{-4}$	$m^2$
$A_2$ , Exit area	$2.38 \times 10^{-3}$	$m^2$
$A_c$ , Chamber cross-sectional area	$5.03 \times 10^{-4}$	$m^2$
$R_t$ , Throat radius	15.23	<i>mm</i>
$R_2$ , Exit radius	27.52	<i>mm</i>
$R_c$ , Chamber radius	40.0	<i>mm</i>
$L_c$ , Chamber length	181.3	<i>mm</i>
$\epsilon$ , Expansion ratio	3.26	<i>N/A</i>
$CR$ , Contraction ratio	6.9	<i>N/A</i>

Table 3: Summary of physical nozzle dimensions.

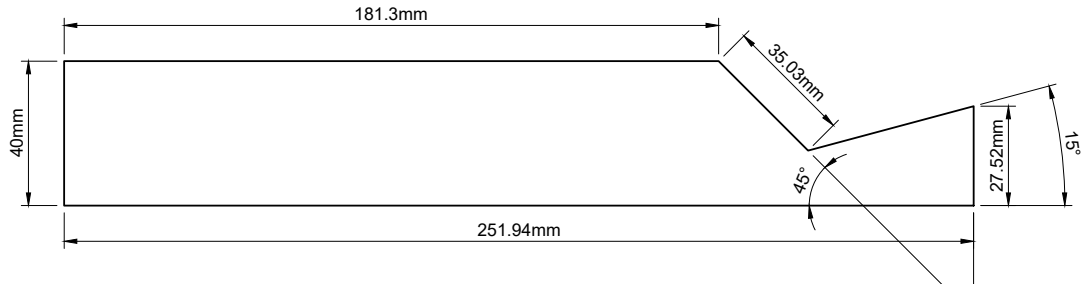


Figure 5: Aphlex 1B drawing with a conical nozzle and given dimensions.

neutralize (reflect in a manner parallel to the nozzle axis) these expansion fans. A MATLAB script was written to execute and create the MOC nozzle, which can be found on our Project Caelus propulsion GitHub repository at <https://github.com/ProjectCaelus/propulsion>. Its output is shown in Figure 6. The Cartesian points representing the generated wall contour were exported as a CSV file, which was then imported into our computer-aided design (CAD) program, Fusion 360, where a best-fit nth-order spline was used to finalize the diverging contour. Although the shape of the nozzle converging section can be optimized significantly, the precise shape of the nozzle converging section has not been found to heavily impact engine performance and is therefore smoothened under the guidelines of Dr. GVR Rao's parabolic approximation method [3][2].

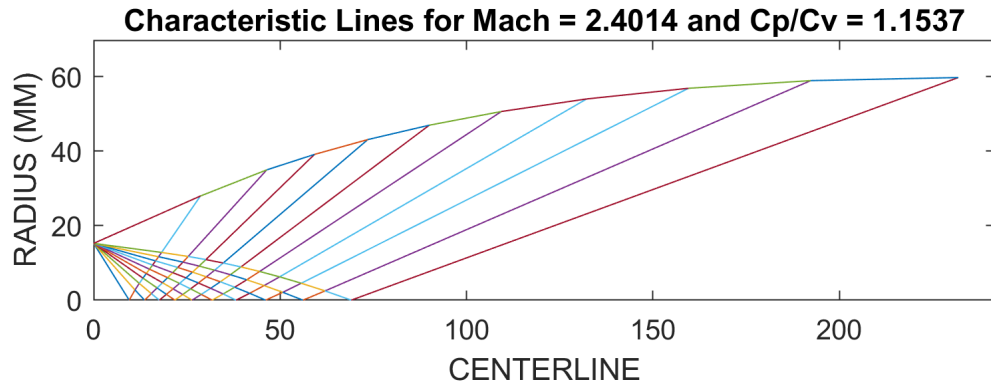


Figure 6: MATLAB visualization for MOC. Shown are the characteristic lines and the generated nozzle contour.

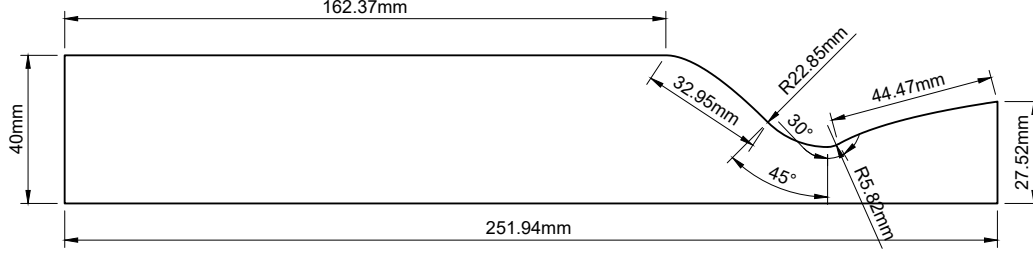


Figure 7: Aphlex 1B drawing with a MOC nozzle and given dimensions.

### 3.2 Injector Design

The injector serves two main purposes in a liquid rocket engine: the adequate mixing (atomization) of the incoming propellant streams to ensure maximum combustion efficiency and the prevention or minimization of combustion instabilities. Some injectors additionally implement film cooling to aid in reducing the thermal load of the chamber and nozzle walls, however, our system relies solely on the heat capacity of the chamber walls and a thin ablative layer to maintain wall integrity. This is done since it would save propellant mass that would otherwise be wasted for film cooling and due to the relatively short burn time of our system.

There are many types of injector elements, each with unique advantages and disadvantages. The injector types considered were the triplet (fuel-centered) unlike impinging injector and the like-on-like doublet impinging injector, due to 1) our limited manufacturing capabilities 2) a fairly unbalanced O/F ratio 3) both types exhibiting good mixing and atomization properties and 4) the abundance of historical experience and data with both injector types. Both the coaxial swirl and pintle types were deemed either too complex to manufacture or too difficult to characterize due to a limited amount of available documentation. NASA's SP-8089 conference document on liquid engine injector design suggests that the best way to characterize both the individual orifice geometries and the overall injector geometry for unlike impinging injectors is through diameter ratios. Vigorous cold flow and other empirically testing methods at the time were used and have found correlations between the driving orifice diameter ratio with the optimum mixing efficiency. The correlation found was

$$\left(\frac{d_c}{d_{ou}}\right)^2 = M \left[ \frac{\rho_{ou}}{\rho_c} \left( \frac{\dot{m}_c}{\dot{m}_{ou}} \right)^2 \right]^{0.7} \quad (3.11)$$

where  $d_c$  is the diameter of center orifice,  $d_{ou}$  is the diameter of an outside individual orifice,  $M$  is an experimentally-determined mixing factor coefficient,  $\rho$  represents liquid density, and  $\dot{m}_c$  and  $\dot{m}_{ou}$  are the center mass flow rate and outside mass flow rate respectively. It is cited that for a 2-on-1 element type,  $M$  has a value of 1.6. Using Equation 3.11, we find that our controlling diameter ratio is

$$\frac{d_c}{d_{ou}} = \sqrt{M \left[ \frac{\rho_{ou}}{\rho_c} \left( \frac{\dot{m}_c}{\dot{m}_{ou}} \right)^2 \right]^{0.7}} = \sqrt{1.6 \left[ \frac{772.25 \text{ kg/m}^3}{789 \text{ kg/m}^3} \left( \frac{0.1389 \text{ kg/s}}{0.5556 \text{ kg/s}} \right)^2 \right]^{0.7}} = 0.4757$$

Since this diameter ratio is not reasonably near 1.22 (as suggested by NASA SP-8089), we can assume this correlation would not be accurate and that there will be potentially drastic losses in mixing efficiency. Thus, this suggests that a like-on-like system is required. Since like-on-like elements will have a 1 to 1 diameter and momentum ratio, we can begin determining the pressure drop and mass flow rate through each individual orifice. Rocket Propulsion Elements (RPE) provides an equation for the volumetric flow rate  $Q$  (and therefore  $\dot{m}$  since  $\rho$  is constant) as shown below:

$$\dot{m} = Q\rho = C_d A \sqrt{2\rho \Delta p} \implies \Delta p = \left[ \left( \frac{\dot{m}}{C_d A} \right)^2 \right] / 2\rho \quad (3.12)$$

where  $C_d$  is a dimensionless discharge coefficient that is experimentally determined and a function of the orifice geometry,  $A$  is the area of the orifice, and  $\Delta p$  is the pressure drop across the orifice. Flow velocity is similar:

$$v = Q/A = C_d \sqrt{2\Delta p / \rho} \quad (3.13)$$

Since  $C_d$  is a measured parameter, initial design calculations must assume a value. RPE suggests a  $C_d$  value of around 0.88 for a 1 mm diameter orifice in a short tube with a rounded entrance (assuming an orifice length to diameter ratio of  $L/D > 3.0$ ), and 0.9 for a similar configuration with a 1.57 mm diameter. Accordingly, a  $C_d$  value of 0.9 was chosen for the oxidizer and a  $C_d$  value of 0.88 was chosen for the fuel. For the orifice sizing, NASA SP-8089 found that smaller orifice sizes attributed to better mixing in all scenarios, although only to a certain extent (orifice diameters  $< 0.03$  inches saw insignificant improvements in mixing). Due to limited manufacturing capabilities, a minimum hole size of 1 mm was chosen. Using this information, a design parameter of an overall injector pressure drop that is 25% of chamber pressure, and Equation 3.12, the mass flow rate across a single oxidizer and fuel orifice are

$$\dot{m}_o = 0.9 * (\pi * ((1.58 \text{ mm}/2) \times 10^{-3})^2) \sqrt{2(772.25 \text{ kg/m}^3)(1.5 \times 10^6 \text{ Pa} * 0.25)} = 0.0425 \text{ kg/s}$$

$$\dot{m}_f = 0.88 * (\pi * ((1.00 \text{ mm}/2) \times 10^{-3})^2) \sqrt{2(789 \text{ kg/m}^3)(1.5 \times 10^6 \text{ Pa} * 0.25)} = 0.0168 \text{ kg/s}$$

The same pressure drops can be used for each orifice due to Bernoulli's principle and the law of conservation of energy, similar to how voltage stays constant across a parallel circuit. The corresponding injection velocities (Equation 3.13) are

$$v_o = 0.9 \sqrt{(2(1.5 \times 10^6 \text{ Pa})(0.25)) / (772.25 \text{ kg/m}^3)} = 28.048 \text{ m/s}$$

$$v_f = 0.88 \sqrt{(2(1.5 \times 10^6 \text{ Pa})(0.25)) / (789 \text{ kg/m}^3)} = 27.132 \text{ m/s}$$

Dividing the mass flow rate by the individual orifice mass flow rates gives the total orifice count for each propellant, denoted as  $n_o$  and  $n_f$ :

$$n_o = \dot{m}_o / \dot{m}_{oi} = (0.4865 \text{ kg/s}) / (0.0425 \text{ kg/s}) = 11.447$$

$$n_f = \dot{m}_f / \dot{m}_{fi} = (0.139 \text{ kg/s}) / (0.0168 \text{ kg/s}) = 8.27$$

Since both an integer and even amount of holes are obviously required for a like-on-like impinging injector, Equation 3.12 is rearranged to compute the necessary diameter given the desired number of orifices, given a reasonable range of orifice count provided by the previous calculation:

$$d = 2 \sqrt{\frac{\dot{m}}{C_d n \pi \sqrt{2 \rho \Delta p}}} \quad (3.14)$$

Solving Equation 3.14 for both oxidizer and fuel streams yields

$$d_o = 2 \sqrt{\frac{0.555 \text{ kg/s}}{(0.9)(16) \pi \sqrt{2(772.25 \text{ kg/m}^3)(1.5 \times 10^6 \text{ Pa})(0.25)}}} = 0.001428 \text{ m} = 1.43 \text{ mm}$$

$$d_f = 2 \sqrt{\frac{0.139 \text{ kg/s}}{(0.88)(8) \pi \sqrt{2(789 \text{ kg/m}^3)(1.5 \times 10^6 \text{ Pa})(0.25)}}} = 0.001017 \text{ m} = 1.02 \text{ mm}$$

Thus, to achieve 16 oxidizer orifices and 8 fuel orifices, an oxidizer orifice diameter of 1.43 mm and fuel orifice diameter of 1.02 mm are needed.

The remaining injector parameters were chosen due to a literature review, rather than explicit calculations. The angle of impingement, also known as the cant angle  $\lambda$ , is defined as the angle between two propellant jets. It was chosen to be 60 degrees since it is the most common impingement angle, prevents significant backslash of propellants onto the injector face (which would produce high heat fluxes with unlike elements), and produces the best atomization characteristics despite requiring a larger  $L^*$ .

NASA SP-8089 further suggests that the free-stream jet length (impingement length), defined as the distance from an element face to the point of impingement, should be somewhere in the range of five to seven times the orifice diameter. In other words,  $5 < L/D \text{ ratio} < 7$ . An  $L/D$  ratio of 6 was chosen, and the free-stream jet length is therefore  $(L_{jet})_o = 6 * 1.43 \text{ mm} = 8.57 \text{ mm}$  and  $(L_{jet})_f = 6 * 1.02 \text{ mm} = 6.10 \text{ mm}$ . The point of impingement (distance of impingement orthogonally measured from the injector face) is therefore  $(L_{POI})_o = 8.57 \cos(30) = 7.42 \text{ mm}$  and  $(L_{POI})_f = 6.10 \cos(30) = 5.28 \text{ mm}$  since the  $\lambda$  half-angle is 30 degrees.

The thickness of the injector plate is driven by the  $L/D$  ratio of the largest orifice (not the jet), which was suggested to be around 10 to ensure smooth and developed flow, assuming the  $C_d$  that was used in previous calculations. Simply,  $L_{inj} = 10(d_{max}) \cos(\lambda/2)$ , since the cosine of the cant half-angle is the



coaxial component (thickness). Evaluating gives  $L_{inj} = (10)(1.42 \text{ mm}) \cos(30) = 12.38 \text{ mm}$ . Finally, finding the distance between each orifice within an element pair involves two separate calculations: one for the distance on the side of the injector face (denoted as “combustor-side”) and one for the distance on its reverse side (denoted as “manifold-side”). First, the combustor-side distance is  $d_{com} = (2)(L_{jet}) \sin(30)$ , and therefore,  $(d_{com})_o = (2)(8.57 \text{ mm}) \sin(30) = 8.57 \text{ mm}$  and  $(d_{com})_f = (2)(6.10 \text{ mm}) \sin(30) = 6.10 \text{ mm}$ . The manifold-side distance is a case of similar triangles with corresponding combustor-side distances:  $(d_{man})_o = [(d_{com})_o / (L_{POI})_o](L_{inj} + (L_{POI})_o) = [8.57 \text{ mm} / 7.42 \text{ mm}](12.38 \text{ mm} + 7.42 \text{ mm}) = 22.87 \text{ mm}$ , and though the complete calculation is not shown here (extreme similarity),  $(d_{man})_f = 20.40 \text{ mm}$ . The final injector parameters are summarized in the table below.

Injector Parameters		
Name	Oxidizer ( $N_2O$ )	Fuel ( $C_2H_5OH$ )
Injector element type	Doublet like-on-like impingement	
$\rho$ , Density at 298 K	$772.25 \text{ kg/m}^3$	$789 \text{ kg/m}^3$
$\dot{m}$ , Mass flow rate	$0.5552 \text{ kg/s}$	$0.1388 \text{ kg/s}$
$C_d$ , Discharge coefficient	0.90	0.88
$n$ , Number of orifices	16	8
$d$ , Orifice diameter	$1.43 \text{ mm}$	$1.02 \text{ mm}$
$A$ , Individual orifice area	$1.61 \times 10^{-6} \text{ m}^2$	$3.27 \times 10^{-6} \text{ m}^2$
Mass flow rate per orifice	$0.0347 \text{ kg/s}$	$0.01735 \text{ kg/s}$
$\lambda$ , Angle of impingement	$60^\circ$	$60^\circ$
$L_{jet}$ , Free-stream jet length	$8.57 \text{ mm}$	$6.10 \text{ mm}$
$L_{POI}$ , Point of impingement	$7.42 \text{ mm}$	$5.28 \text{ mm}$
Length of orifice	$14.28 \text{ mm}$	$10.16 \text{ mm}$
$d_{com}$ , Distance between orifices (combustor)	$8.57 \text{ mm}$	$6.10 \text{ mm}$
$d_{man}$ , Distance between orifices (manifold)	$22.87 \text{ mm}$	$20.40 \text{ mm}$
$L_{inj}$ , Injector plate thickness	$12.38 \text{ mm}$	

Table 4: Summary of injector parameters.

The physical configuration of the injector and the element pattern were chosen qualitatively. A standard two-ring pattern was implemented, with the outer ring consisting of No baffles or other dampening devices were utilized since the chamber is small enough to neglect large-scale instabilities.

[Do a sanity check that the  $\Delta p$  across injector is between 5 % and 25 %, according to MASA and 8089 pp. 35 (44 on PDF)].

### 3.3 Plumbing System Design

The plumbing system was designed with key considerations in mind which would make the system as versatile and safe as possible in the event of errors or hardware problems. The first of these was that all pressurization and post-pressurization actions must be done remotely. Furthermore, the system must be able to vent pressure and drain propellant both remotely and manually. Finally, the system must have adequate redundancy where it is necessary to ensure safety. Figure 7 displays the full piping and instrumentation diagram for the Aphlex 1B cold flow test. The following subsections will go into detail on the different parts of the plumbing system.

#### 3.3.1 Ethanol Fill and Pressurization System

The ethanol fill and pressurization use the same inlet in order to save costs and avoid purchasing unnecessary hardware. Ethanol will be poured manually into the tank since it is safe and not toxic, cryogenic, or at a high pressure where it might pose danger to someone manually handling it. During this time both MBV-1 and NCSV-1 will be open Once this is complete, the Nitrogen K-bottle will be connected to the rest of the piping system,

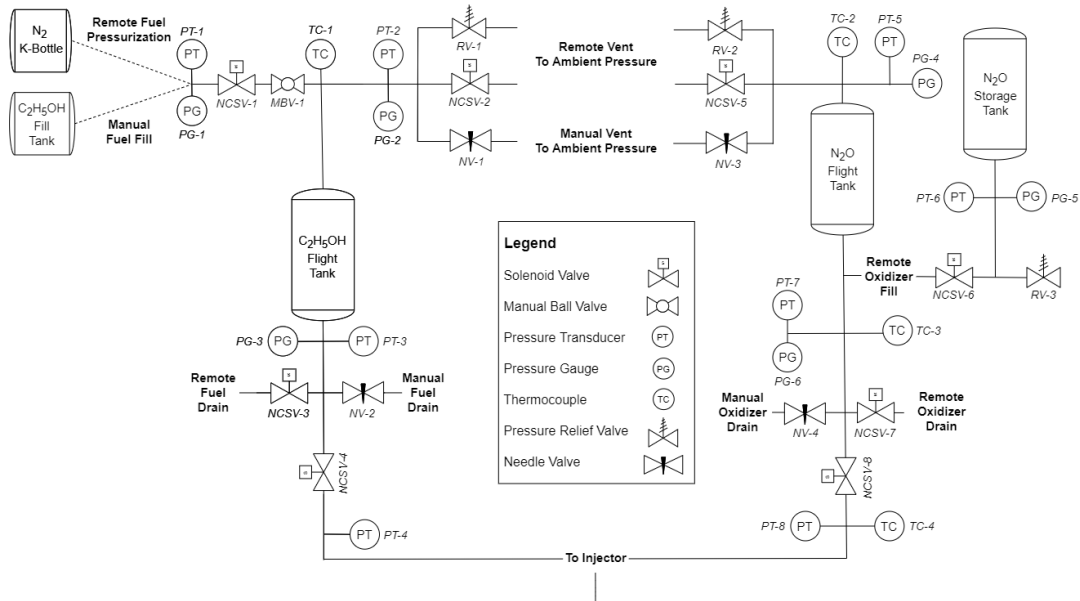


Figure 8: Full System Piping and Instrumentation Diagram

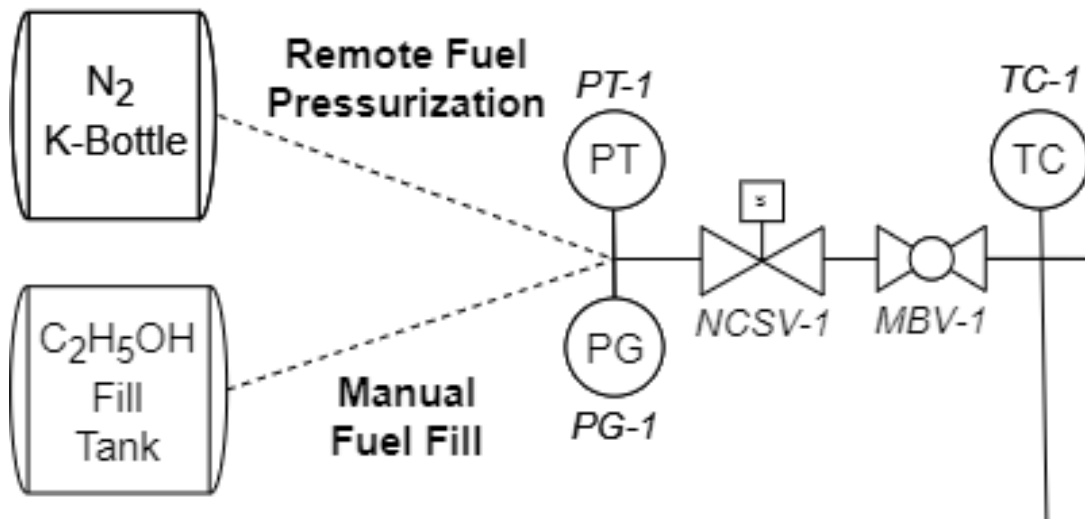


Figure 9: Fill System

## 4 Ethanol Cold Flow Test Stand Design

## 5 Launch Vehicle Design

### 5.1 Objectives

### 5.2 Callisto 1

## References

- [1] Tomasz Palacz. "Nitrous Oxide Application for Low-Thrust and Low-Cost Liquid Rocket Engine". In: *7th European Conference for Aeronautics and Space Sciences* (July 2017).

- [2] GVR Rao. “Exhaust Nozzle Contour for Optimum Thrust”. In: *Jet Propulsion Archive* 28.6 (June 1958).
- [3] George P. Sutton and Oscar Biblarz. *Rocket Propulsion Elements, 9th Edition*. Wiley, Dec. 2016.